Biochemical and Biophysical Research Communications 404 (2011) 528–533

Contents lists available at ScienceDirect

Biochemical and Biophysical Research Communications

journal homepage: www.elsevier.com/locate/ybbrc

Pou3f4 deficiency causes defects in otic fibrocytes and stria vascularis by different mechanisms

Mee Hyun Song [a,b,1], Soo-Young Choi [c,1], Ling Wu [b,d,1], Se-Kyoung Oh [c], Hee Keun Lee [c], Dong Jin Lee [d], Dae-Bo Shim [a,b], Jae Young Choi [b], Un-Kyung Kim [c], Jinwoong Bok [d,*]

[a] Department of Otorhinolaryngology, Kwandong University College of Medicine, Goyang 412-270, South Korea
[b] Department of Otorhinolaryngology, Yonsei University College of Medicine, Seoul 120-752, South Korea
[c] Department of Biology, Kyungpook National University, Daegu 702-701, South Korea
[d] Department of Anatomy, BK21 Project for Medical Science, Yonsei University College of Medicine, Seoul 120-752, South Korea

ARTICLE INFO

Article history:
Received 29 November 2010
Available online 7 December 2010

Keywords:
Pou3f4
Transcription factor
DFN3
Hearing loss

ABSTRACT

DFN3, the most prevalent X-linked hearing loss, is caused by mutations in the *POU3F4* gene. Previous studies in *Pou3f4* knockout mice suggest that defective otic fibrocytes in the spiral ligament of the cochlear lateral wall may underlie the hearing loss in DFN3. To better understand the pathological mechanisms of the DFN3 hearing loss, we analyzed inner ears of *Pou3f4*-deficient mice during development. Our results indicate that compartmentalization of the spiral ligament mesenchyme setting up boundaries for specific otic fibrocytes occurs normally in *Pou3f4*-deficient cochlea. However, differentiation of the compartmentalized mesenchyme into specific otic fibrocytes was blocked in the absence of Pou3f4 function. In addition, we found that stria vascularis in the cochlear lateral wall was also affected in *Pou3f4*-deficient cochlea. Unlike the otic fibrocytes, differentiation of stria vascularis was completed in the absence of Pou3f4 function, yet expression of Kir4.1 channels in the strial intermediate cells, essential for the sound transduction, was lost afterwards. These results suggest that *Pou3f4* deficiency causes defects in both otic fibrocytes and stria vascularis at different developmental stages and by different pathological mechanisms, which may account for the progressive nature of DFN3 hearing loss.

1. Introduction

X-linked deafness type 3 (DFN3) is the most prevalent X-linked hereditary form of hearing loss [1,2]. DFN3 is caused by mutations in the *POU3F4* gene, which encodes a POU family transcription factor. Mutations identified in DFN3 patients have been shown to abolish the transcriptional activity of POU3F4 proteins [3], suggesting that the hearing loss in DFN3 patients is caused by mis-regulation of genes important for inner ear development or function. *Pou3f4,* the mouse orthologue of the *POU3F4* gene, is expressed in the periotic mesenchyme surrounding the developing inner ear epithelium [4]. During early development, the periotic mesenchyme is compartmentalized into two zones; the outer zone is condensed and differentiated into the bony otic capsule protecting the inner ear epithelium, while the inner zone forms other mesenchyme-derived cochlear structures including the spiral ligament located between the otic capsule and the inner ear epithelium [4]. The spiral ligament mesenchyme is again compartmentalized and differentiated into five distinct types of otic fibrocytes depending on their locations and unique gene expression patterns (See below; Fig. 2A)[4,5]. The otic fibrocytes play critical roles in the sound transduction by providing a mesenchymal gap junction network essential for ion homeostasis in the cochlea [5,6].

Mouse models for DFN3 have been generated by targeted mutagenesis or by spontaneous mutations in the *Pou3f4* locus [7–10]. These *Pou3f4*-deficient mice are profoundly deaf and display anomalies in the mesenchyme-derived structures such as the temporal bones and spiral ligament, consistent with the expression domains of *Pou3f4* [7–10]. Analysis of the spiral ligament of *Pou3f4*-deficient mice by transmission electron microscopy revealed severe ultrastructural alterations of the otic fibrocytes [7]. Immunohistochemical analyses further showed that expressions of fibrocyte-specific proteins were either lost or misplaced in *Pou3f4*-deficient cochlea [10,11]. These fibrocyte defects have been considered a major cause of the DFN3 hearing loss, yet it is currently unclear when and how the otic fibrocytes become defective in the *Pou3f4*-deficient mice. In addition, since the hearing impairments in DFN3 patients are often progressive [2], there may be other cochlear defects besides the otic fibrocytes, which could explain the progressiveness of DFN3 hearing loss.

* Corresponding author. Address: Department of Anatomy, Yonsei University College of Medicine, Seoul 120-752, South Korea. Fax: +82 2 365 0700.
E-mail address: bokj@yuhs.ac (J. Bok).
[1] These authors contributed equally to this work.

0006-291X/$ - see front matter © 2010 Elsevier Inc. All rights reserved.
doi:10.1016/j.bbrc.2010.12.019

To better understand the pathological mechanisms of DFN3 hearing loss, we analyzed the inner ears of *Pou3f4del-J* mice, a model for DFN3, during development. Our data suggest that *Pou3f4* deficiency causes defects not only in the otic fibrocytes but also in the stria vascularis, both of which are essential for the sound transduction of the cochlea, by different pathological mechanisms.

2. Materials and methods

2.1. Animal and deletion analysis

C3HeB/FeJ–Pou3f4$^{del\text{-}J}$*/J (Pou3f4del-J)* mice were purchased from The Jackson Laboratory (ME, USA). Experimental procedures were approved by the Animal Care and Use Committee of Yonsei University College of Medicine. For deletion analysis, total 39 primer pairs were used for PCR amplification of the genomic DNAs of wild type and mutant animals. STS markers were selected to amplify the regions of interest, and additional primer pairs were designed from the non-repetitive unique sequence (<http://frodo.wi.mit.edu/>; <http://www.repeatmasker.org/cgi-bin/WEBRepeatMasker>). Representative primer pairs shown in Fig. 1 were 107.53 (5′-ACTTG TGTCTAGTTTGTTCTCTCTT-3′ and 5′-ATTAGTTGTAGAAGGAAGTAC CC-3′), 107.542 (5′-CAAAGGTCACACCCATAGCAT-3′ and 5′-ATAGGC CTCCATCCACTCACT-3′), Pou3f4 (5′-TGAGTGTCAAGGGCGTACTG-3′ and 5′-AGGCGCTGAAAGGTTATTCA-3′), 108.071 (5′-AGTGTCAGG GGGTGGTAAATC-3′ and 5′-CAAAATCCATTTAGGGCCTGT-3′), and 108.1 (5′-AATGGTTCTGAATGGGGTAGG-3′ and 5′-CAGCTTGCCTC AAGAAGTGAA-3′). Specificity of the amplified PCR products was confirmed by direct sequencing.

2.2. Measurement of auditory brainstem response

Auditory brainstem responses (ABR) were obtained with TDT workstation (Tucker–Davis Technologies, Alachua, FL, USA). ABR testing was conducted in a tailored double-walled sound chamber for animal models. ABR threshold was defined as the lowest intensity of stimulation required to attain repeatable ABR wave V.

2.3. Histologic analysis, Immunohistochemistry, and in-situ hybridization

For histological analysis, the inner ears were dissected after intracardiac perfusion with 4% paraformaldehyde and kept in 4% paraformaldehyde overnight at 4 °C. After rinsing with 0.01 M phosphate buffer saline, the specimens were decalcified in 0.5 M EDTA/PBS for 48 h, dehydrated with ethanol, and embedded in paraffin. Serial sections of 5 μm thickness were prepared in the midmodiolar plane and subjected to hematoxylin–eosin (HE) staining or immunofluorescent labeling. Immunofluorescent labeling was performed as previously reported [12]. Antibodies used were anti-Aquaporin1 (Millipore #AB3272), anti-Connexin26 (Zymed #71-0500), anti-Na^+–K^+–ATPase α-1 (Millipore #06-520), anti-

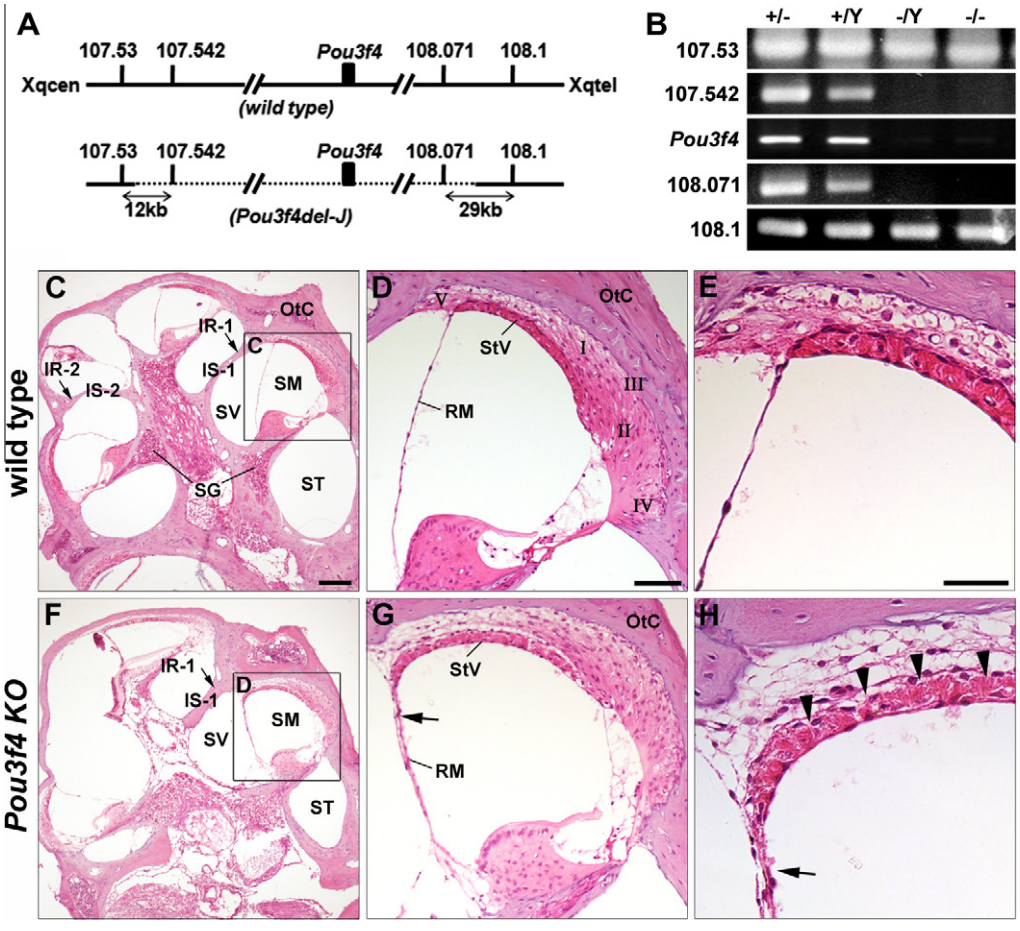

Fig. 1. *Pou3f4del-J* mice as a model for DFN3. (A) Schematic representation of wild type and *Pou3f4del-J* mutant genome. Dotted line represents the deleted region. Vertical bars indicate the primer sets used in PCR reactions in (B). (C–H) Hematoxylin & eosin staining of the mid-modiolar sections of the cochlea in wild type (C–E) and *Pou3f4*-deficient mutant (F–H) at P21. (C and F) Defective modiolus in *Pou3f4*-deficient cochlea. (D, E, G and H) Type IV and V otic fibrocytes are lost in the *Pou3f4*-deficient spiral ligament. Stria vascularis shows decreased cellular density (arrowheads) and Reissner's membrane is less flattened in the mutants (arrow). *IR*, interscalar ridge; *IS*, interscalar septum; *OtC*, otic capsule; *RM*, Reissner's membrane; *SM*, scala media; *ST*, scala tympani; *StV*, stria vascularis; *SV*, scala vestibuli. Scale bars: in (C) 100 μm for (C and F) in (D), 50 μm for (D and G), in (E), 25 μm for (E and H).

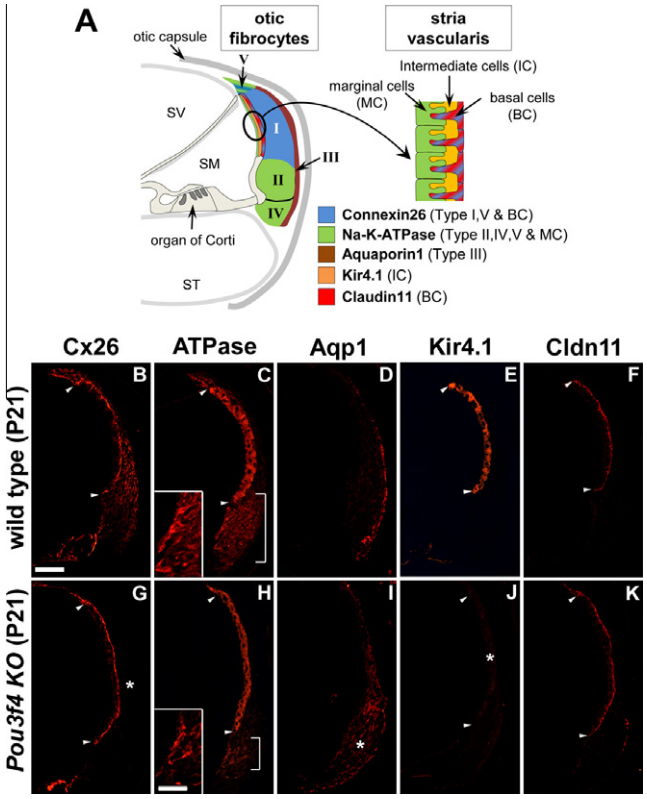

Fig. 2. Defects of otic fibrocytes and stria vascularis in *Pou3f4*-defecient cochlea at P21. (A) Schematic illustration indicating expression domains of specific markers for otic fibrocytes and stria vascularis. (B and G) Cx26 expression is lost in type I and V fibrocyte regions of the spiral ligament (asterisk), but not in the stria vascularis, in *Pou3f4*-deficient cochlea. (C and H) Na–K–ATPase expression is greatly reduced in type II and V fibrocyte regions of the spiral ligament (H, bracket), but not in the stria vascularis (H, arrowheads), in *Pou3f4*-deficient cochlea. Magnified views suggest that the reduced Na–K–ATPase expression is observed mainly in root cell processes (insets). (D and I) Aquaporin1, normally restricted in type III fibrocytes located between otic capsule and spiral ligament (D), is dispersed broadly in the entire spiral ligament in *Pou3f4*-deficient cochlea (I, asterisk). (E and J) Kir4.1 expression in the intermediate cells of stria vascularis (arrowheads) is lost in *Pou3f4*-deficient cochlea (asterisk). (F and K) Normal expression of Claudin11 in the basal cells of wild type and mutant cochleae (arrowheads). Cx26 (Connexin26), ATPase (Na–K–ATPase), Aqp1 (Aquaporin1), Cldn11 (Claudin11). Scale bar in (B), 100 μm for all panels.

Kir4.1 (Alomone labs #APC-035), anti-Claudin11 (Zymed #36-4500). *In-situ* hybridization was performed as previously described [13]. Riboprobes for *Trp2* [14], *Cx26* and *E-cad* [4] were prepared as previously described. Riboprobes for *Crym* were generated from a 382 bp mouse *Crym* cDNA fragment containing −46 to +336 nucleotides (NM_016669), and for *Ecrg4*, from a 520 bp mouse *Ecrg4* cDNA containing the entire open reading frame as well as 34 bp 5′ and 39 bp 3′ untranslated regions (NM_024283).

3. Results and discussion

3.1. Pou3f4del-J mice as an animal model for DFN3 hearing loss

Pou3f4del-J mice identified by typical behaviors associated with inner ear abnormalities at The Jackson Laboratory were known to carry a spontaneous deletion in the *Pou3f4* locus and have been used as a mouse model lacking Pou3f4 function (<http://mousemutant.jax.org/articles/pou3f4del.html>) [15,16]. Our detailed analysis on the break points of the genome revealed a large deletion of approximately 550 kb including the *Pou3f4* gene, which is larger than previously suggested (<http://mousemutant.jax.org/articles/pou3f4del.html>). The deletion breakpoints were approximately 470 kb upstream and 70 kb downstream of the *Pou3f4* gene (Fig. 1). There exist three hypothetical genes in the deleted region besides the *Pou3f4*, none of which are likely associated with ear development or hearing function. We also confirmed the hearing loss of *Pou3f4del-J* hemizygous males ($n = 4$) by auditory brainstem response (ABR) at weaning (postnatal day 21; P21).

Analysis of gross cochlear morphology of the *Pou3f4del-J* mutants showed similar abnormalities to those exhibited in *Pou3f4* knockout mice (Fig. 1C–H)[8,10,11]. Bony structures in the modiolus were severely affected, and scala tympani of the basal turn is smaller in volume compared to controls (Fig. 1C and F). Mesenchymal cells located lateral to the basilar membrane (type IV fibrocyte area) and those located above the stria vascularis (type V fibrocyte area) were lost (Fig. 1D and G; Fig. 2A). Stria vascularis seemed less densely populated (Fig. 1E and H, arrowheads) and the Reissner's membrane was less flattened in *Pou3f4del-J* mutants (Fig. 2D–H, arrows).

We next examined the defects of otic fibrocytes in *Pou3f4del-J* mutants at P21, when the mice suffer profound hearing loss. In wild types, otic fibrocytes are classified into five distinct types according to their locations and gene expression patterns (Fig. 2A). Type I fibrocytes, located near stria vascularis, express Connexin26 (Cx26), a gap junction protein important for ionic homeostasis (Fig. 2B), while Type II and IV fibrocytes, located lateral to the spiral prominence and basilar membrane, respectively, express Na–K–ATPase, important for K^+ ion recycling (Fig. 2C) [17]. Type V fibrocytes, located above stria vascularis, express both Cx26 and Na–K–ATPase (Fig. 2A–C). Type III fibrocytes, located between the spiral ligament and otic capsule, express Aquaporin1 (Aqp1), a water transporter protein (Fig. 2A and D)[18]. In *Pou3f4-del-J* mutants, these fibrocyte-specific expressions patterns were either lost (Cx26, Na–K–ATPase) or misplaced (Aqp1) (Fig. 2G–I), while their expressions in stria vascularis were largely unaffected (Fig. 2B, C, G and H, arrowheads). These results show that the *Pou3f4del-J* spontaneous mutants closely recapitulate the cochlear phenotypes observed in *Pou3f4* knockout models [7,10,11], and also indicate that all types of otic fibrocytes are severely affected in the absence of Pou3f4 function.

3.2. Developmental defects of otic fibrocytes in Pou3f4-deficient mice

To elucidate the pathological mechanisms of the fibrocyte defects, we examined the inner ears of *Pou3f4del-J* mice during development. At P1, Cx26 expression was observed in the mesenchyme near the differentiating stria vascularis (Fig. 3A). This expression domain became condensed and finally restricted in the lining of the basal cells of stria vascularis by P12 (Fig. 3B and C), suggesting that the cells expressing Cx26 at these stages contribute mainly to the basal cells of stria vascularis but not to the otic fibrocytes. At P12, another wave of Cx26 expression began in the spiral ligament near and above the stria vascularis, indicative of differentiation of type I and V fibrocytes (Fig. 3C, arrows). This second wave of Cx26 expression was completely blocked in *Pou3f4*-deficient cochlea (Fig. 3G, asterisk), resulting in defective type I and V otic fibrocytes (Fig. 2G).

Expression of Na–K–ATPase at P12 was mainly observed in the epithelial structures such as the marginal cells of stria vascularis (Fig. 3I and M, arrowheads) and the root cell processes (Fig. 3I and M, insets) in both wild type and mutant cochlea. Na–K–ATPase expression was strongly up-regulated in the spiral ligament during the next few days in wild types (Fig. 2C, bracket)[17], but no such upregulation was observed in *Pou3f4*-deficient mutants (Fig. 2H, brackets), resulting in defective type II and IV otic fibrocytes (Fig. 2H).

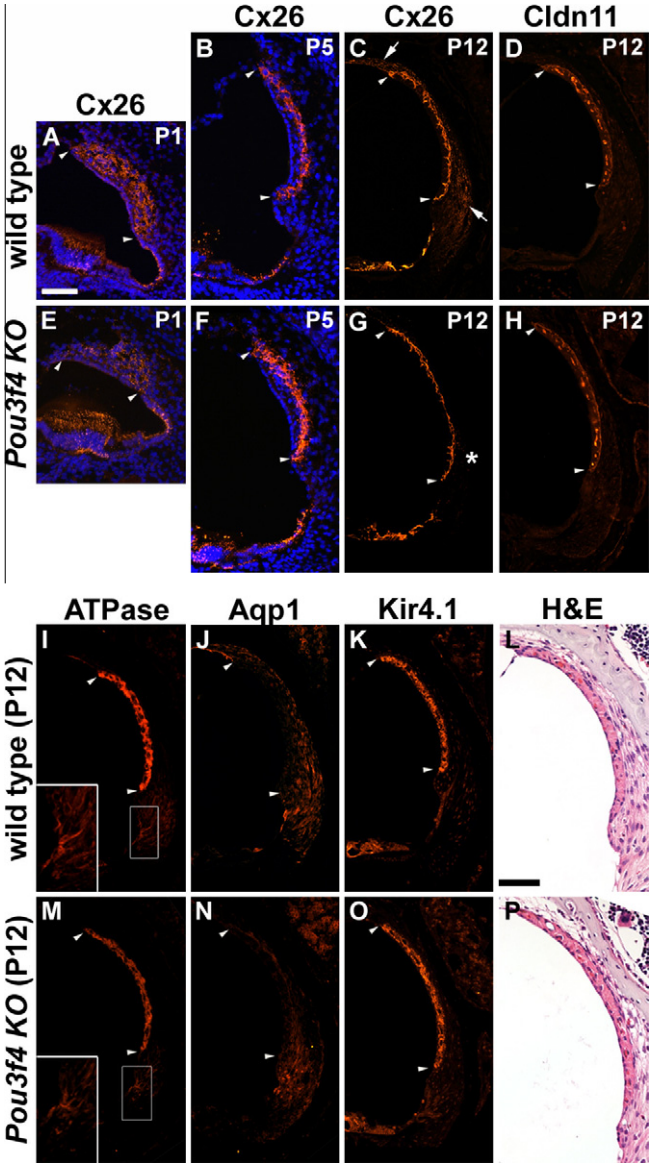

Fig. 3. Neonatal development of otic fibrocytes and stria vascularis in *Pou3f4*-defecient cochlea. Developmental processes of otic fibrocytes and stria vascularis of wild type (A–D, I–L) and *Pou3f4*-deficient mice (E–H, M–P). (A–C, E–G) Cx26 expression patterns in the condensing mesenchyme differentiating into the basal cells of stria vascularis at P1 (A and E), P5 (B and F), and P12 (C and G). Arrowheads indicate the presumptive stria vascularis. At P12, Cx26 expressions in type I and V fibrocyte regions (arrows) are observed in wild type but not in *Pou3f4*-deficient cochlea (asterisk). (D and H) Expression patterns of Cldn11 in basal cells of stria vascularis are similar between wild type and mutant at P12 (arrowheads). (I and M) Expression patterns of Na–K–ATPase in marginal cells of stria vascularis (arrowheads) and root cell processes (insets) are similar between wild type and mutant cochlea. (J and N) Aqp1 expression is observed broadly in the entire spiral ligament of both wild type and mutant cochlea at P12. (K and O) Kir4.1 expression patterns in intermediate cells of stria vascularis look normal in mutant cochlea at P12 (arrowheads). (L and P) Histological appearance of stria vascularis of wild type and mutant cochlea at P12. Scale bars: in A, 100 μm for A–K, M–O; in L, 50 μm for L and P.

In addition, we found that Aqp1, normally expressed at the border between the bony capsule and spiral ligament in adult cochlea (Fig. 2A and D), was initially expressed in the entire spiral ligament at P12 (Fig. 3J and N). While this broad expression domain became restricted to the type III fibrocyte region during the next few days in wild types (Fig. 2D), such restriction did not occur in the mutants (Fig. 2I).

Together, these results suggest that differentiation of the spiral ligament into specific otic fibrocytes is severely affected at around P12 in *Pou3f4*-deficient cochlea.

3.3. Mesenchymal compartmentalization in the developing spiral ligament of Pou3f4-deficient cochlea

Abnormal differentiation of the otic fibrocytes in *Pou3f4*-deficient mice may indicate that mesenchymal compartmentalization in the spiral ligament, which sets up boundaries for each otic fibrocyte, be affected in *Pou3f4*-deficient cochlea. To test this possibility, we examined expression patterns of genes that show the mesenchymal compartmentalization of the spiral ligament prior to expression of otic fibrocyte-specific genes.

Crym encoding μ-crystallin has been shown mainly expressed in type II and IV fibrocytes [19,20]. However, we found that *Crym* was initially expressed in the entire spiral ligament during embryonic development (Fig. 4A), and later restricted to type II and IV fibrocyte regions by P1 (Fig. 4B). In addition, we identified that expression of *Ecrg4* (*Esophageal cancer-related gene 4*) is associated with type I fibrocyte region in the spiral ligament mesenchyme

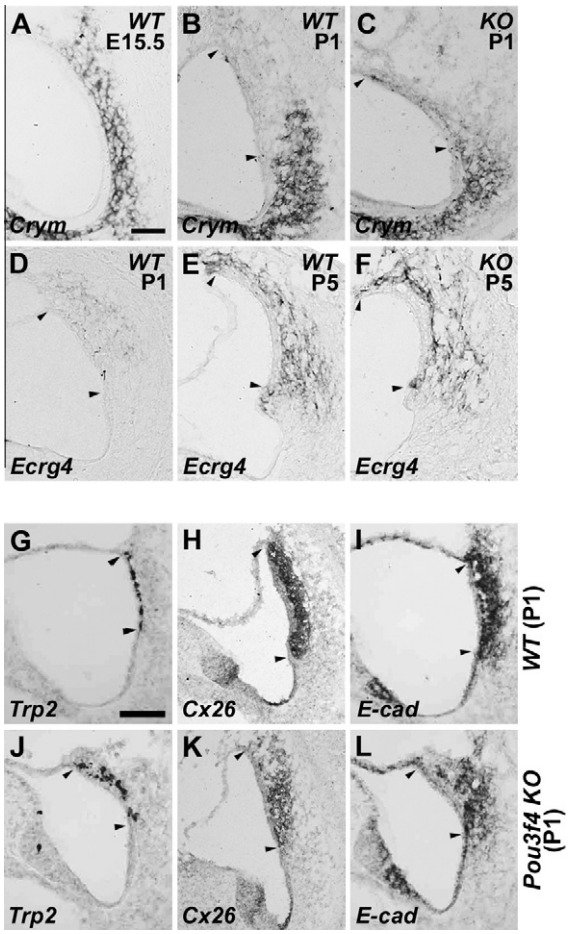

Fig. 4. Gene expression analyses in the neonatal cochlea of *Pou3f4*-deficient mice. (A–C) *Crym* is expressed in the entire spiral ligament at E15.5 (A), but is restricted to the type II/IV fibrocyte regions by P1 (B). Similar restricted expression of *Crym* is also obvious in *Pou3f4*-deficient spiral ligament (C). (D–F) *Ecrg4* expression begins in the type I fibrocyte region at P1 (D) and the restricted expression pattern gets stronger at P5 (E). Similar restricted expression of *Ecrg4* is observed in *Pou3f4*-deficient spiral ligament (F). (G and J) Cells expressing *Trp2* are more scattered in *Pou3f4*-deficient mutants compared to those in controls at P1 (J, arrowheads). (H, I, K and L) Expressions of *Cx26* and *E-cad* in the differentiating basal cells are weaker and more scattered in the mutants compared to controls at P1. Arrowheads in all panels indicate the border of presumptive stria vascularis. Scale bar; in A, 50 μm for A–F; in G, 50 μm for G–L.

(Fig. 4D and E). *Ecrg4* encodes a secreted protein that has recently been implicated in cell senescence and cartilage development [21,22], yet its role in the inner ear is currently unknown. Unlike *Crym*, *Ecrg4* expression began specifically in the type I fibrocyte region at around P1 (Fig. 4D), when the broad expression of *Crym* became restricted in the type II/IV fibrocyte region (Fig. 4B). These complementary expression patterns of *Crym* and *Ecrg4* at neonatal stages indicate that the spiral ligament mesenchyme becomes compartmentalized well before the expression of fibrocyte-specific proteins. Using these genes as markers, we asked whether the defective fibrocyte differentiation in *Pou3f4*-deficient cochlea was due to abnormal compartmentalization of the spiral ligament mesenchyme. We observed that expressions of both *Crym* and *Ecrg4* were generally unaffected in the *Pou3f4*-deficient spiral ligament (Fig. 4C and F). These results suggest that mesenchymal compartmentalization establishing boundaries for each fibrocytes occurs normally in the absence of Pou3f4, but their subsequent differentiation into mature fibrocytes (e.g. expression of fibrocyte-specific genes) is severely affected.

Currently, downstream targets of Pou3f4 in the spiral ligament important for fibrocyte differentiation are unknown. Thus far, only a few genes have been reported to be involved in fibrocyte differentiation including *Otospiralin (Otos)* and *Tbx18* [4,23]. However, neither *Otos* nor *Tbx18* expression is affected in the developing spiral ligament of *Pou3f4*-deficient mice (data not shown), indicating that the fibrocyte defects in *Pou3f4*-deficient mice are not due to mis-regulation of *Otos* or *Tbx18* expression. Currently, we are investigating the genes misregulated in the spiral ligament of *Pou3f4*-deficient cochlea by microarray analysis. Identification of direct downstream targets of Pou3f4 will help elucidating molecular mechanisms of how Pou3f4 contributes to differentiation of otic fibrocytes.

3.4. Defects of stria vascularis in Pou3f4-deficient mice

We next examined the stria vascularis of *Pou3f4*-deficient cochlea, which showed decreased cellular integrity (Fig. 1H)[10]. Stria vascularis is a multilayer structure composed of three distinct cell types derived from different origins (Fig. 2A); marginal cells facing the scala media are originated from the otic epithelium, basal cells facing the spiral ligament are differentiated through mesenchymal–epithelial transition, and intermediate cells located between the marginal and basal cells are neural crest melanocytes migrating from the dorsal part of the neural tube.

Expression patterns of Na–K–ATPase in the stria vascularis of *Pou3f4*-deficient cochlea (Figs. 2A, C, H and 3I,M) suggest that the epithelium-derived marginal cells do not require Pou3f4 function for its normal development. Consistently, *Bsnd*, encoding chloride channels localized in the marginal cells [24], was expressed normally in neonatal mutant cochlea (data not shown). Even though *Pou3f4* is expressed in the mesenchymal region where a mesenchymal–epithelial transition occurs to form the basal cells, the basal cells were normal in *Pou3f4*-deficient cochlea, based on the expression patterns of Cx26 (Figs. 2B, G and 3A–C, E–G) and Claudin11 (Cldn11; Figs. 2F, K and 3D and H). By contrast, expression of Kir4.1, an inward rectifier potassium channel, in intermediate cells [25], was not observed in *Pou3f4*-deficient cochlea at P21 (Fig. 2A, E and J, asterisk). Since Kir4.1 is known to be responsible for the generation of endocochlear potential (EP), which is essential for the sound transduction [26], the Kir4.1 loss may be the direct cause of EP reduction observed in *Pou3f4*-deficient mice [7] and possibly of the sensorineural hearing loss in DFN3 patients.

To better understand the pathological mechanism of the Kir4.1 loss, we examined differentiation processes of the strial intermediate cells in *Pou3f4*-deficient mice. *Trp2*, encoding a melanogenic enzyme DOPAchrome tautomerase [14], was used as a marker for migrating melanocytes (intermediate cells). At P1, *Trp2* expressing cells were more scattered near the prospective stria vascularis in *Pou3f4*-deficient mutants compared to those in wild types (Fig. 4G and J, arrowheads), suggesting a delay in migration of the neural crest cells in *Pou3f4*-deficient cochlea. Consistently, mesenchymal expression of *Cx26* and *E-cadherin (E-cad)* near the prospective stria vascularis, suggestive of the mesenchymal–epithelial transition leading to basal cell differentiation [4], were also weaker and broader in the mutants (Fig. 4H, I, K and L). However, the delay appeared to be caught up by P12, when expression patterns of Cx26/Cldn11 in basal cells (Fig. 3C, D, G and H) and Kir4.1 in intermediate cells (Fig. 3K and O) became indistinguishable between wild type and *Pou3f4*-deficient cochlea. Histological appearance of the mutant stria vascularis also looked normal at P12 (Fig. 3L and P), suggesting that differentiation of stria vascularis can be completed in the absence of Pou3f4 function with a slight delay.

However, Kir4.1 expression in the intermediate cells was lost in a next few days by P17 (Fig. 2J; data not shown), which was unexpected because *Pou3f4* is not expressed in the migrating neural crest or differentiated intermediate cells. Similar loss of Kir4.1 in the intermediate cells has been reported in mice lacking *Slc26a4*, coding for the HCO_3^- transporter pendrin, and free radical stress has been suggested responsible for the Kir4.1 loss [27,28]. Interestingly, in both *Pou3f4*- and *Slc26a4*-deficient mice, the Kir4.1 loss occurs between P10 and P17, when the generation of a small endocochlear potential begins and rapidly increases to the adult level [28]. Whether similar pathological mechanism leads to the Kir4.1 loss in *Pou3f4*- and *Slc26a4*-deficient cochlea is yet to be determined. Nevertheless, this observation provides the Kir4.1 loss, in addition to the defective otic fibrocytes, as a possible cause of the hearing loss in DFN3.

Taken together, our results demonstrate that *Pou3f4* deficiency causes defects in otic fibrocytes and stria vascularis, both of which are essential for the sound transduction, at different stages and by different mechanisms, which may account for the progressive nature of the DFN3 hearing loss.

Acknowledgments

We thank Mr. Byoungki Yoo for technical assistance and Dr. Andreas Kispert for providing probes for in situ hybridization. This work is supported by Korea Healthcare Technology R&D Project, Ministry for Health, Welfare and Family Affairs, Republic of Korea (A084906).

References

[1] Y.J. de Kok, S.M. van der Maarel, M. Bitner-Glindzicz, I. Huber, A.P. Monaco, S. Malcolm, M.E. Pembrey, H.H. Ropers, F.P. Cremers, Association between X-linked mixed deafness and mutations in the POU domain gene POU3F4, Science 267 (1995) 685–688.
[2] M.B. Petersen, Q. Wang, P.J. Willems, Sex-linked deafness, Clin. Genet. 73 (2008) 14–23.
[3] H.K. Lee, M.H. Song, M. Kang, J.T. Lee, K.A. Kong, S.J. Choi, K.Y. Lee, H. Venselaar, G. Vriend, W.S. Lee, H.J. Park, T.K. Kwon, J. Bok, U.K. Kim, Clinical and molecular characterizations of novel POU3F4 mutations reveal that DFN3 is due to null function of POU3F4 protein, Physiol. Genom. 39 (2009) 195–201.
[4] M.O. Trowe, H. Maier, M. Schweizer, A. Kispert, Deafness in mice lacking the T-box transcription factor Tbx18 in otic fibrocytes, Development 135 (2008) 1725–1734.
[5] S.S. Spicer, B.A. Schulte, Differentiation of inner ear fibrocytes according to their ion transport related activity, Hear Res. 56 (1991) 53–64.
[6] T. Kikuchi, J.C. Adams, Y. Miyabe, E. So, T. Kobayashi, Potassium ion recycling pathway via gap junction systems in the mammalian cochlea and its interruption in hereditary nonsyndromic deafness, Med. Electron. Microsc. 33 (2000) 51–56.
[7] O. Minowa, K. Ikeda, Y. Sugitani, T. Oshima, S. Nakai, Y. Katori, M. Suzuki, M. Furukawa, T. Kawase, Y. Zheng, M. Ogura, Y. Asada, K. Watanabe, H. Yamanaka, S. Gotoh, M. Nishi-Takeshima, T. Sugimoto, T. Kikuchi, T. Takasaka, T. Noda,

Altered cochlear fibrocytes in a mouse model of DFN3 nonsyndromic deafness, Science 285 (1999) 1408–1411.
[8] D. Phippard, L. Lu, D. Lee, J.C. Saunders, E.B. Crenshaw 3rd, Targeted mutagenesis of the POU-domain gene Brn4/Pou3f4 causes developmental defects in the inner ear, J. Neurosci. 19 (1999) 5980–5989.
[9] D. Phippard, Y. Boyd, V. Reed, G. Fisher, W.K. Masson, E.P. Evans, J.C. Saunders, E.B. Crenshaw 3rd, The sex-linked fidget mutation abolishes Brn4/Pou3f4 gene expression in the embryonic inner ear, Hum. Mol. Genet. 9 (2000) 79–85.
[10] E.M. Braunstein, E.B. Crenshaw III, B.E. Morrow, J.C. Adams, Cooperative function of Tbx1 and Brn4 in the periotic mesenchyme is necessary for cochlea formation, J. Assoc. Res. Otolaryngol. 9 (2008) 33–43.
[11] A.P. Xia, T. Kikuchi, O. Minowa, Y. Katori, T. Oshima, T. Noda, K. Ikeda, Late-onset hearing loss in a mouse model of DFN3 non-syndromic deafness: morphologic and immunohistochemical analyses, Hear. Res. 166 (2002) 150–158.
[12] X.H. Wang, M. Streeter, Y.P. Liu, H.B. Zhao, Identification and characterization of pannexin expression in the mammalian cochlea, J. Comp. Neurol. 512 (2009) 336–346.
[13] H. Morsli, D. Choo, A. Ryan, R. Johnson, D.K. Wu, Development of the mouse inner ear and origin of its sensory organs, J. Neurosci. 18 (1998) 3327–3335.
[14] K.P. Steel, D.R. Davidson, I.J. Jackson, TRP-2/DT, a new early melanoblast marker, shows that steel growth factor (c-kit ligand) is a survival factor, Development 115 (1992) 1111–1119.
[15] S.M. Jones, K.R. Johnson, H. Yu, L.C. Erway, K.N. Alagramam, N. Pollak, T.A. Jones, A quantitative survey of gravity receptor function in mutant mouse strains, J. Assoc. Res. Otolaryngol. 6 (2005) 297–310.
[16] Y. Nakano, S.H. Kim, H.M. Kim, J.D. Sanneman, Y. Zhang, R.J. Smith, D.C. Marcus, P. Wangemann, R.A. Nessler, B. Banfi, A claudin-9-based ion permeability barrier is essential for hearing, PLoS Genet. 5 (2009) e1000610.
[17] A. Xia, T. Kikuchi, K. Hozawa, Y. Katori, T. Takasaka, Expression of connexin 26 and Na, K-ATPase in the developing mouse cochlear lateral wall: functional implications, Brain Res 846 (1999) 106–111.
[18] J. Li, A.S. Verkman, Impaired hearing in mice lacking aquaporin-4 water channels, J. Biol. Chem. 276 (2001) 31233–31237.
[19] S. Usami, Y. Takumi, N. Suzuki, T. Oguchi, A. Oshima, H. Suzuki, R. Kitoh, S. Abe, A. Sasaki, A. Matsubara, The localization of proteins encoded by CRYM, KIAA1199, UBA52, COL9A3, and COL9A1, genes highly expressed in the cochlea, Neuroscience 154 (2008) 22–28.
[20] S. Abe, T. Katagiri, A. Saito-Hisaminato, S. Usami, Y. Inoue, T. Tsunoda, Y. Nakamura, Identification of CRYM as a candidate responsible for nonsyndromic, deafness, through cDNA microarray analysis of human cochlear and vestibular tissues, Am. J. Hum. Genet. 72 (2003) 73–82.
[21] Y.H. Huh, J.H. Ryu, S. Shin, D.U. Lee, S. Yang, K.S. Oh, C.H. Chun, J.K. Choi, W.K. Song, J.S. Chun, Esophageal cancer related gene 4 (ECRG4) is a marker of articular chondrocyte differentiation and cartilage destruction, Gene 448 (2009) 7–15.
[22] Y. Kujuro, N. Suzuki, T. Kondo, Esophageal cancer-related gene 4 is a secreted inducer of cell senescence expressed by aged CNS precursor cells, Proc. Natl. Acad. Sci. USA 107 (2010) 8259–8264.
[23] B. Delprat, J. Ruel, M.J. Guitton, G. Hamard, M. Lenoir, R. Pujol, J.L. Puel, P. Brabet, C.P. Hamel, Deafness and cochlear fibrocyte alterations in mice deficient for the inner ear protein otospiralin, Mol. Cell Biol. 25 (2005) 847–853.
[24] R. Birkenhager, E. Otto, M.J. Schurmann, M. Vollmer, E.M. Ruf, I. Maier-Lutz, F. Beekmann, A. Fekete, H. Omran, D. Feldmann, D.V. Milford, N. Jeck, M. Konrad, D. Landau, N.V. Knoers, C. Antignac, R. Sudbrak, A. Kispert, F. Hildebrandt, Mutation of BSND causes Bartter syndrome with sensorineural deafness and kidney failure, Nat. Genet. 29 (2001) 310–314.
[25] M. Ando, S. Takeuchi, Immunological identification of an inward rectifier K+ channel (Kir4.1) in the intermediate cell (melanocyte) of the cochlear stria vascularis of gerbils and rats, Cell Tissue Res. 298 (1999) 179–183.
[26] D.C. Marcus, T. Wu, P. Wangemann, P. Kofuji, KCNJ10 (Kir4.1) potassium channel knockout abolishes endocochlear potential, Am. J. Physiol. Cell Physiol. 282 (2002) C403–407.
[27] P. Wangemann, E.M. Itza, B. Albrecht, T. Wu, S.V. Jabba, R.J. Maganti, J.H. Lee, L.A. Everett, S.M. Wall, I.E. Royaux, E.D. Green, D.C. Marcus, Loss of KCNJ10 protein expression abolishes endocochlear potential and causes deafness in Pendred syndrome mouse model, BMC Med. 2 (2004) 30.
[28] R. Singh, P. Wangemann, Free radical stress-mediated loss of Kcnj10 protein expression in stria vascularis contributes to deafness in Pendred syndrome mouse model, Am. J. Physiol. Renal Physiol. 294 (2008) F139–148.